

DIFFUSION PROCESS OF LARGE RANDOM MATRICES *

EWA GUDOWSKA-NOWAK^{a,b}, ROMUALD A. JANIK^b
JERZY JURKIEWICZ^b AND MACIEJ A. NOWAK^{a,b}

^a Gesellschaft für Schwerionenforschung
Planckstrasse 1, 64291 Darmstadt, Germany

^b M. Smoluchowski Institute of Physics, Jagellonian University
Reymonta 4, 30-059 Kraków, Poland

(Received September 5, 2003)

We describe a matrix analogy of the log-normal random walk, in the large N (size of the matrix) limit. In particular, we present an exact result for the infinite product of random matrices, corresponding to the multiplicative diffusion triggered by Ginibre–Girko ensemble. We observe the emergence of a “topological phase transition”, when a hole develops in the complex eigenvalue spectrum, after some critical diffusion time τ_{crit} is reached.

PACS numbers: 05.40.+j, 05.45+b, 05.70.Fh, 11.15.Pg

1. Introduction

Random matrix theory represents a powerful tool in several statistical problems, when the degrees of freedom could be encoded as elements of certain ensembles of large matrices. Examples of applications of random matrix theory (RMT) in physics range from interpretation of complex spectra of energy levels in atomic and nuclear physics [1], studies of disordered systems [2,3], chaotic behavior [4], Euclidean Quantum Chromodynamics [5] and supersymmetric Yang–Mills theories [6] to quantum gravity [7–9]. Progressively developed methods of RMT turned out to be also useful in other sciences such as meteorology [10], image processing [11], population ecology [12] or economy [13–15].

Most of the applications of random matrices correspond to the case, when the dynamics of the systems is assumed to be “static”. On the other hand one often considers systems which evolve w.r.t. some external parameter τ

* Presented at the Workshop on Random Geometry, Kraków, Poland, May 15–17, 2003.

(“time”). The “time parameter” can represent either real time or another parameter like length or surface of some samples, or the inverse of the temperature, or rapidity etc. The infinitesimal, matrix-valued increments could be of additive or multiplicative nature, and the matrices may be in general complex, hermitian, unitary etc, generated by various probability distributions.

Such processes constitute a rich class of stochastic evolutions, but analytical results in the “dynamical” random matrix theory are still rather scarce, although numerous applications exist. Some solved or partially solved examples in physics include the localization of electronic wave functions in random potentials [2, 17], applications of infinite product of random matrices (hereafter PRM) to the analysis of chaotic dynamical systems [16, 18–20], dynamics of Yang–Mills theory on various manifolds [21], and evolution of linear chains of interacting hermitian matrices [22]. There are also several examples of multiplicative, matrix-valued processes in applied physics and interdisciplinary research, ranging from the studies of stability of large eco- and social- systems [12], adaptive algorithms and the analysis of system performance under the influence of external noises [23] to image compression [24, 25] and communication via antenna arrays [26, 27].

In this talk we present an effective calculational technique for studying products of random matrices in the large N limit, and use these tools to derive the properties of the natural matrix valued generalization of the geometric (multiplicative) diffusion type process. The scalar versions of these processes, leading to log-normal distributions are ubiquitous in various fields [28].

In particular, we are interested in properties of the *matrix-valued evolution operator* defined as

$$Y(\tau) = \lim_{M \rightarrow \infty} \left[\left(1 + \mu \frac{\tau}{M} + \sigma \sqrt{\frac{\tau}{M}} X_1 \right) \left(1 + \mu \frac{\tau}{M} + \sigma \sqrt{\frac{\tau}{M}} X_2 \right) \dots \right. \\ \left. \dots \left(1 + \mu \frac{\tau}{M} + \sigma \sqrt{\frac{\tau}{M}} X_M \right) \right], \quad (1)$$

where μ is some deterministic “drift” matrix and the stochastic matrices X_i belong to identical independent random matrix ensembles, belonging to Girko–Ginibre ensembles, *i.e.* complex Gaussian ensembles. In particular we will be studying the eigenvalue distribution of $Y(\tau)$:

$$\rho_\tau(z) = \frac{1}{N} \left\langle \text{tr} \delta^{(2)}(z - Y(\tau)) \right\rangle, \quad (2)$$

where the average is taken over stochastic N by N matrices X_i appearing in the definition of $Y(\tau)$ and $\delta^{(2)}$ is a complex Dirac delta function.

If the variable X_i would be a random *number* from Gaussian distribution and μ would be also a number, we would recover the conventional (scalar) multiplicative (geometric) random walk in one dimension in the presence of some external (constant) drift force. The process belongs to the class of (Markovian) Ito diffusion processes, whose stochastic variable y undergoes an evolution

$$\frac{dy}{y} = \mu d\tau + \sigma dx_\tau. \tag{3}$$

In the above stochastic differential equation (SDE), dx_τ represents the Wiener process (integral of the Gaussian white-noise), respecting

$$\langle dx_\tau \rangle = 0, \quad \langle dx_\tau^2 \rangle = d\tau. \tag{4}$$

We use here small letters in our notation to avoid confusion with similar, but matrix-valued entries, represented by capital letters. After averaging $y(\tau)$ over the independent identical distributions (iid) of the Gaussian variables x_i and taking the limit $M \rightarrow \infty$, we recover¹ the well known solution for the probability density of $y(\tau)$:

$$p(y, \tau | y_0, 0) = \frac{1}{y\sqrt{2\pi\sigma^2\tau}} \exp \left[-\frac{(\log(y/y_0) - \mu\tau + \frac{1}{2}\sigma^2\tau)^2}{2\sigma^2\tau} \right] \tag{5}$$

with y restricted to positive values.

A direct analogue of the scalar solution (5) is the τ -dependent eigenvalue distribution (2). In this talk we would like to describe methods developed in [44] leading to the determination of (2).

The problem is much harder than in the scalar case. Indeed in order to understand the statistical properties of the spectra of the *operator* $Y(\tau)$ as a function of evolution time τ we have to overcome two problems: first, since the matrices X_i in general do not commute, we are dealing with a ‘path ordered product’. Second, even if the matrices X_i are hermitian, their product is not, *i.e.* the spectrum in general disperses into the complex plane, showing — as later pointed out in this talk — some rather unusual feature described as a “topological phase transition”. Namely the support of the eigenvalue distribution changes from a simply-connected two-dimensional island to a two-dimensional island with a hole.

We will solve the evolution problem of operator (1) in three steps, which we call *diagrammatization*, *complex replication* and *cyclization*, respectively.

¹ The log-normal distribution $y(\tau)$ is easy to infer looking at the form of the product. Taking the logarithm, expanding and using the central limit theorem we immediately see, that the r.h.s. tends to the Gaussian distribution.

In order to make this presentation self-contained, in the next section we recall the diagrammatical formalism for hermitian RMM, basically in order to define our notation and conventions. Then, we address the problem of finding the eigenvalue distribution of nonhermitian random matrix ensembles, with complex spectrum, and we recall our earlier construction (complex replication), originating from the extension of diagrammatic methods to the non-hermitian case [31,32]. As an example we will use the complex Gaussian non-hermitian random matrix model, considered in this paper as a source of the matrix diffusion.

Finally, as the third step, we will introduce a trick named by us (borrowing from chemistry²) *cyclization*, which will allow us to linearize the problem of studying the spectral properties of infinite product (1).

Last chapter concludes the paper and points some other interesting consequences of the formalism presented here.

2. Diagrammatization

A key problem in random matrix theories is to find the distribution of eigenvalues λ_i , in the large N (size of the matrix H) limit, *i.e.*

$$\rho(\lambda) = \frac{1}{N} \left\langle \sum_{i=1}^N \delta(\lambda - \lambda_i) \right\rangle, \quad (6)$$

where the averaging $\langle \dots \rangle$ is done over the ensemble of $N \times N$ random hermitian matrices generated with probability

$$P(H) \propto e^{-N\text{Tr}V(H)}. \quad (7)$$

The eigenvalues of course lie on the real axis. By introducing the resolvent (Green's function)

$$G(z) = \frac{1}{N} \left\langle \text{Tr} \frac{1}{z - H} \right\rangle. \quad (8)$$

with $z = z\mathbf{1}_N$ and by using the standard relation

$$\frac{1}{\lambda \pm i\varepsilon} = \text{P.V.} \frac{1}{\lambda} \mp i\pi\delta(\lambda). \quad (9)$$

the spectral function (6) can be derived from the discontinuities of the Green's function (8)

² Cyclization — formation of cyclic structures (rings) in a chemical compound.

$$\begin{aligned} \frac{1}{2\pi i} \lim_{\varepsilon \rightarrow 0} (G(\lambda - i\varepsilon) - G(\lambda + i\varepsilon)) &= \frac{1}{N} \langle \text{Tr} \delta(\lambda - H) \rangle \\ &= \frac{1}{N} \left\langle \sum_{i=1}^N \delta(\lambda - \lambda_i) \right\rangle = \rho(\lambda). \end{aligned} \tag{10}$$

There are several ways of calculating Green’s functions for HRMM [1, 3, 9]. Here we follow the diagrammatic approach, after [29]. A starting point of the approach is the expression allowing for the reconstruction of the Green’s function from all the moments $\langle \text{Tr} H^n \rangle$,

$$\begin{aligned} G(z) &= \frac{1}{N} \left\langle \text{Tr} \frac{1}{z - H} \right\rangle = \frac{1}{N} \left\langle \text{Tr} \left[\frac{1}{z} + \frac{1}{z} H \frac{1}{z} + \frac{1}{z} H \frac{1}{z} H \frac{1}{z} + \dots \right] \right\rangle \\ &= \frac{1}{N} \sum_n \frac{1}{z^{n+1}} \langle \text{Tr} H^n \rangle. \end{aligned} \tag{11}$$

The reason why the above procedure works correctly for *hermitian* matrix models is the fact that the Green’s function is guaranteed to be *holomorphic* in the whole complex plane except at most on one or more 1-dimensional intervals. We will use the diagrammatic method to evaluate efficiently the sum of the moments on the right hand side. We will now restrict ourselves to the well known case of a random hermitian ensemble with a Gaussian distribution.

The first step is to introduce a generating function with a matrix-valued source J :

$$Z(J) = \int dH e^{-\frac{N}{2}(\text{Tr} H^2) + \text{Tr} H \cdot J}, \tag{12}$$

where we integrate over all N^2 elements of the matrix H . All moments follow directly from $Z(J)$ through the relation

$$\langle \text{Tr} H^n \rangle = \frac{1}{Z(0)} \text{Tr} \left(\frac{\partial}{\partial J} \right)^n Z(J) \Big|_{J=0} \tag{13}$$

and are straightforward to calculate, since in the Gaussian case the partition function (12) reads $Z(J) = \exp \frac{1}{2N} \text{Tr} J^2$. Accordingly, the lowest nonzero expectation value is

$$\langle H_b^a H_d^c \rangle = \frac{\partial^2 Z(J)}{\partial J_a^b \partial J_c^d} \Big|_{J=0} = \frac{1}{N} \frac{\partial J_d^c}{\partial J_a^b} \Big|_{J=0} = \frac{1}{N} \delta_b^c \delta_d^a \tag{14}$$

and the next non-vanishing expectation value reads

$$\langle H_b^a H_d^c H_f^e H_h^g \rangle = \frac{1}{N^2} \left(\delta_b^c \delta_d^a \delta_f^g \delta_h^e + \delta_h^a \delta_g^b \delta_f^c \delta_e^d + \delta_f^a \delta_e^b \delta_h^c \delta_g^d \right). \tag{15}$$

The key idea in the diagrammatic approach is to associate to the expressions for the moments, like the one above, a graphical representation following from a simple set of rules. The power of the approach is that it enables to perform a resummation of the whole power series (11) through the identification of the structure of the relevant graphs.

We depict the “Feynman” rules in Fig. 1, similar to the standard large N diagrammatics for QCD [30]. The $1/z = 1/z\delta_a^b$ in (11) is represented by a horizontal straight line. The propagator (14) is depicted as a double line.

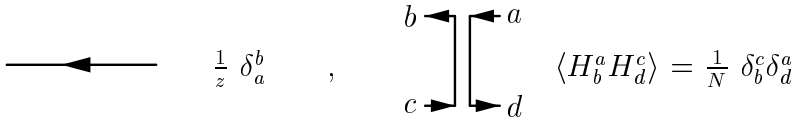


Fig. 1. Large N “Feynman” rules for “quark” and “gluon” propagators.

The diagrammatic expansion of the Green’s function is visualized in Fig. 2, where one connects the vertices with the double line propagators in all possible ways. Each “propagator” brings a factor of $1/N$, and each loop a factor of $\delta_a^a = N$. From the three terms, corresponding to (15) contributing to $\langle \text{tr } H^4 \rangle$ only the first two are presented in Fig. 2 (the third and the fourth diagram). The diagram corresponding to the third term in (15) represents a non-planar contribution which is suppressed as $1/N^2$ and hence vanishes when $N \rightarrow \infty$. In general, only planar graphs survive the large N limit.

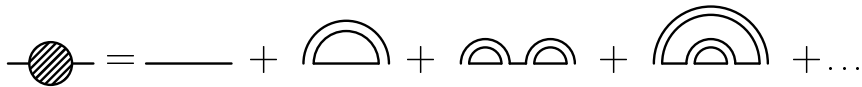


Fig. 2. Diagrammatic expansion of the Green’s function up to the $O(H^4)$ terms.

The resummation of (11) is done by introducing the self-energy Σ comprising the sum of all one-particle irreducible graphs (rainbow-like). Then the Green’s function reads

$$G(z) = \frac{1}{z - \Sigma(z)}. \tag{16}$$

In the large N limit the equation for the self energy Σ , follows from resumming the rainbow-like diagrams of Fig. 2. The resulting equation

(“Schwinger–Dyson” equation of Fig. 3) encodes pictorially the structure of these graphs and reads

$$\Sigma = \frac{1}{N} \text{Tr} G \mathbf{1} = \frac{N}{N} G = G. \tag{17}$$

Equations (16) and (17) give immediately $G(z - G) = 1$ which can be solved to yield

$$G_{\mp}(z) = \frac{1}{2}(z \mp \sqrt{z^2 - 4}). \tag{18}$$

Only the G_- is a normalizable solution, with the proper asymptotic behavior $G(z) \rightarrow 1/z$ in the $z \rightarrow \infty$ limit. From the discontinuity (cut), using (10), we recover Wigner’s semicircle [33] for the distribution of the eigenvalues for hermitian random matrices

$$\rho(\lambda) = \frac{1}{2\pi} \sqrt{4 - \lambda^2}. \tag{19}$$

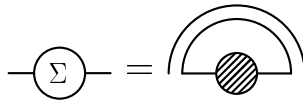


Fig. 3. Schwinger–Dyson equation for rainbow diagrams.

3. Complex replication

The main difficulty in the treatment of non-hermitian random matrix models is the fact that now the eigenvalues accumulate in *two-dimensional* domains in the complex plane and the Green’s function is no longer holomorphic. Therefore the power series expansion (11) no longer captures the full information about the Green’s function. In particular the eigenvalue distribution is related to the non-analytic (non-holomorphic) behavior of the Green’s function:

$$\frac{1}{\pi} \partial_z G(z) = \rho(z). \tag{20}$$

This phenomenon can be easily seen even in the simplest non-hermitian ensemble — the Ginibre–Girko one [34, 35], with non-hermitian matrices X , and measure

$$P(X) = e^{-N \text{Tr} X X^\dagger}. \tag{21}$$

It is easy to verify that all moments vanish $\langle \text{tr } X^n \rangle = 0$, for $n > 0$ so the expansion (11) gives the Green’s function to be $G(z) = 1/z$ (diagrammatically this follows from the fact that the propagator $\langle X_b^a X_d^c \rangle$ vanishes and hence the self-energy $\Sigma = 0$). The true answer is, however, different. Only for $|z| > 1$ one has indeed $G(z) = 1/z$. For $|z| < 1$ the Green’s function is nonholomorphic and equals $G(z) = \bar{z}$.

The above difficulty was first addressed in mathematical papers. Brown [36] defined a measure for complex ensembles as

$$\mu_X = \frac{1}{2\pi} \left(\frac{\partial^2}{(\partial \Re \lambda)^2} + \frac{\partial^2}{(\partial \Im \lambda)^2} \right) \log \det(X - \lambda), \tag{22}$$

where

$$\det(X - \lambda) = \exp \left[\frac{1}{N} \text{Tr} \log \sqrt{(X - \lambda)(X^\dagger - \lambda^*)} \right] \tag{23}$$

is known in mathematics as Fuglede–Kadison determinant. For some recent results on Brown measure we refer to [37, 38].

Physicists have addressed the problem of measure, exploiting the analogy to two-dimensional electrostatics [4, 35, 39]. Let us define the “electrostatic potential”

$$F = \frac{1}{N} \text{Tr} \ln[(z - \mathcal{M})(\bar{z} - \mathcal{M}^\dagger) + \varepsilon^2]. \tag{24}$$

Then

$$\begin{aligned} \lim_{\varepsilon \rightarrow 0} \frac{\partial^2 F(z, \bar{z})}{\partial z \partial \bar{z}} &= \lim_{\varepsilon \rightarrow 0} \frac{1}{N} \left\langle \text{Tr} \frac{\varepsilon^2}{(|z - \mathcal{M}|^2 + \varepsilon^2)^2} \right\rangle \\ &= \frac{\pi}{N} \left\langle \sum_i \delta^{(2)}(z - \lambda_i) \right\rangle \equiv \pi \rho(x, y) \end{aligned} \tag{25}$$

represents Gauss law, where $z = x + iy$. The last equality follows from the representation of the complex Dirac delta

$$\pi \delta^{(2)}(z - \lambda_i) = \lim_{\varepsilon \rightarrow 0} \frac{\varepsilon^2}{(\varepsilon^2 + |z - \lambda_i|^2)^2}. \tag{26}$$

In the spirit of the electrostatic analogy we can define the Green’s function $G(z, \bar{z})$, as an “electric field”

$$G \equiv \frac{\partial F}{\partial z} = \frac{1}{N} \lim_{\varepsilon \rightarrow 0} \left\langle \text{Tr} \frac{\bar{z} - X^\dagger}{(\bar{z} - X^\dagger)(z - X) + \varepsilon^2} \right\rangle. \tag{27}$$

Then Gauss law reads

$$\partial_{\bar{z}}G = \pi\rho(x, y) \tag{28}$$

leading to the eigenvalue density $\rho(z, \bar{z})$.

Both constructions (Brown measure, Green’s function (27)) are however difficult to use in practical calculation.

Instead of working *ab initio* with the object (27), and in view of applying diagrammatic methods it is much more convenient to proceed differently — as we will now discuss.

Following [31] we define the matrix-valued resolvent through

$$\begin{aligned} \hat{\mathcal{G}} &= \frac{1}{N} \left\langle \text{Tr}_{\text{B2}} \left(\begin{array}{cc} z - X & i\varepsilon \\ i\varepsilon & \bar{z} - X^\dagger \end{array} \right)^{-1} \right\rangle \\ &= \frac{1}{N} \left\langle \text{Tr}_{\text{B2}} \left(\begin{array}{cc} A & B \\ C & D \end{array} \right) \right\rangle \equiv \begin{pmatrix} \mathcal{G}_{\text{I1}} & \mathcal{G}_{\text{I}\bar{\text{I}}} \\ \mathcal{G}_{\bar{\text{I}}\text{I}} & \mathcal{G}_{\bar{\text{I}}\bar{\text{I}}} \end{pmatrix} \end{aligned} \tag{29}$$

with

$$\begin{aligned} A &= \frac{\bar{z} - X^\dagger}{(\bar{z} - X^\dagger)(z - X) + \varepsilon^2}, \\ B &= \frac{-i\varepsilon}{(z - X)(\bar{z} - X^\dagger) + \varepsilon^2}, \\ C &= \frac{-i\varepsilon}{(\bar{z} - X^\dagger)(z - X) + \varepsilon^2}, \\ D &= \frac{z - X}{(z - X)(\bar{z} - X^\dagger) + \varepsilon^2} \end{aligned} \tag{30}$$

and where we introduced the ‘block trace’ defined as

$$\text{Tr}_{\text{B2}} \left(\begin{array}{cc} A & B \\ C & D \end{array} \right)_{2N \times 2N} \equiv \begin{pmatrix} \text{Tr } A & \text{Tr } B \\ \text{Tr } C & \text{Tr } D \end{pmatrix}_{2 \times 2}. \tag{31}$$

Then, by definition, the upper-right component \mathcal{G}_{I1} , is equal to the Green’s function (27).

The block approach has several advantages. First of all it is *linear* in the random matrices X allowing for a simple diagrammatic calculational procedure. Let us define $2N$ by $2N$ matrices

$$\mathcal{Z} = \begin{pmatrix} z & i\varepsilon\mathbf{1} \\ i\varepsilon\mathbf{1} & \bar{z} \end{pmatrix}, \quad \mathcal{H} = \begin{pmatrix} X & 0 \\ 0 & X^\dagger \end{pmatrix}. \tag{32}$$

Then the generalized Green’s function is given formally by the same definition as the usual Green’s function G ,

$$\mathcal{G} = \frac{1}{N} \left\langle \text{Tr}_{\text{B2}} \frac{1}{\mathcal{Z} - \mathcal{H}} \right\rangle. \tag{33}$$

What is more important, also in this case the Green’s function is completely determined by the knowledge of all matrix-valued moments

$$\langle \text{Tr}_{\text{B2}} \mathcal{Z}^{-1} \mathcal{H} \mathcal{Z}^{-1} \mathcal{H} \dots \mathcal{Z}^{-1} \rangle. \tag{34}$$

This last observation allows for a diagrammatic interpretation. The Feynman rules are analogous to the hermitian ones, only now one has to keep track of the block structure of the matrices, *e.g.* single straight lines will now be associated with a *matrix* factor \mathcal{Z}^{-1} . We will now demonstrate the above procedure by solving diagrammatically the complex Gaussian Random Matrix Model.

As an example of the complex replication procedure outlined above, we consider the Ginibre–Girko ensemble, defined by the measure

$$P(X) \propto e^{-N \text{Tr} X X^\dagger}. \tag{35}$$

In this case the double line propagators are

$$\begin{aligned} \langle X_b^a X_d^c \rangle &= \langle X_b^{\dagger a} X_d^{\dagger c} \rangle = 0, \\ \langle X_b^a X^{\dagger c} \rangle &= \langle X_b^{\dagger a} X_d^c \rangle = \frac{1}{N} \delta_d^a \delta_c^b. \end{aligned} \tag{36}$$

As previously, we introduce a self-energy $\tilde{\Sigma}$, (but which is now matrix-valued), in terms of which we get a two by two matrix expression

$$\mathcal{G} = (\mathcal{Z} - \tilde{\Sigma})^{-1}, \tag{37}$$

where the 2 by 2 matrix \mathcal{Z} reads

$$\mathcal{Z} = \begin{pmatrix} z & i\varepsilon \\ i\varepsilon & \bar{z} \end{pmatrix}. \tag{38}$$

The resummation of the rainbow diagrams for $\tilde{\Sigma}$ is more subtle, but follows easily from the structure of the propagators (36). The analogue of (17) is now:

$$\tilde{\Sigma} \equiv \begin{pmatrix} \Sigma_{11} & \Sigma_{1\bar{1}} \\ \Sigma_{\bar{1}1} & \Sigma_{\bar{1}\bar{1}} \end{pmatrix} = \begin{pmatrix} 0 & \mathcal{G}_{1\bar{1}} \\ \mathcal{G}_{\bar{1}1} & 0 \end{pmatrix}. \tag{39}$$

The two by two matrix equations (37)–(39) completely determine the problem of finding the eigenvalue distribution for the Girko–Ginibre ensemble. Inserting (39) into (37) we get:

$$\begin{pmatrix} \mathcal{G}_{11} & \mathcal{G}_{1\bar{1}} \\ \mathcal{G}_{\bar{1}1} & \mathcal{G}_{\bar{1}\bar{1}} \end{pmatrix} = \frac{1}{|z|^2 - \mathcal{G}_{1\bar{1}}\mathcal{G}_{\bar{1}1}} \cdot \begin{pmatrix} \bar{z} & \mathcal{G}_{1\bar{1}} \\ \mathcal{G}_{\bar{1}1} & z \end{pmatrix}. \tag{40}$$

Note that at this moment we can safely put to zero the regulators ε . Looking at the off-diagonal equation

$$\mathcal{G}_{1\bar{1}} = \frac{\mathcal{G}_{1\bar{1}}}{|z|^2 - \mathcal{G}_{1\bar{1}}\mathcal{G}_{\bar{1}1}} \tag{41}$$

we see that there are two solutions: one with $\mathcal{G}_{1\bar{1}} = 0$, and another with $\mathcal{G}_{1\bar{1}} \neq 0$. The first one leads to a holomorphic Green’s function, and a straightforward calculation gives

$$G(z) = \frac{1}{z}. \tag{42}$$

The second one is nonholomorphic, imposing the condition

$$|z|^2 - b^2 = 1, \tag{43}$$

where we denoted $\mathcal{G}_{1\bar{1}}\mathcal{G}_{\bar{1}1} \equiv b^2$, hence

$$G(z, \bar{z}) = \bar{z} \tag{44}$$

which leads, via the Gauss law, to

$$\rho(x, y) = \frac{1}{\pi} \frac{\partial}{\partial \bar{z}} G(z, \bar{z}) = \frac{1}{\pi}. \tag{45}$$

Both solutions match at the boundary $b^2 = 0$, which in this case reads $z\bar{z} = 1$. In such a simple way we recovered the results of Ginibre and Girko for the complex non-hermitian ensemble. The eigenvalues are uniformly distributed on the unit disk $|z|^2 < 1$.

This example illustrates more general properties of the matrix valued generalized Green’s function. Each component of the matrix carries important information about the stochastic properties of the system. There are always two solutions for \mathcal{G}_{11} , one holomorphic, another non-holomorphic. The second one leads, via Gauss law, to the eigenvalue distribution. The shape of the “coastline” bordering the “sea” of complex eigenvalues is determined by the matching conditions for the two solutions, *i.e.* it is determined by imposing on the non-holomorphic solution for b^2 the equation $b^2 = 0$. $\mathcal{G}_{1\bar{1}}\mathcal{G}_{\bar{1}1} \equiv b^2$ is also related to the properties of *eigenvector* statistics in the nonhermitian random matrix model [42]. For other important features of the explained above diagrammatic method, their link to Free Random Variables calculus [40, 41] and more complex examples see [31, 42, 43].

4. Cyclization

We consider now the product of an arbitrary number of matrices (1). To see the pattern, let us look briefly at the case of three matrices

$$\begin{aligned}
 Y_3 &= \left(1 + \sqrt{\frac{\tau}{3}}X_1\right) \left(1 + \sqrt{\frac{\tau}{3}}X_2\right) \left(1 + \sqrt{\frac{\tau}{3}}X_3\right) \\
 &\equiv A_1A_2A_3,
 \end{aligned}
 \tag{46}$$

where X_1, X_2, X_2 again belong to the Girko–Ginibre ensemble.

Our approach again follows from a very simple *exact* relation between the eigenvalues of a product of $N \times N$ matrices $A_1A_2A_3$ and the eigenvalues of a block matrix

$$\mathcal{B}_3 = \begin{pmatrix} 0 & A_1 & 0 \\ 0 & 0 & A_2 \\ A_3 & 0 & 0 \end{pmatrix}_{3N \times 3N}.
 \tag{47}$$

Indeed if $\{\lambda_i\}$ are the eigenvalues of $A_1A_2A_3$ then the eigenvalues of the block matrix are $\{\lambda_i^{1/3}, \lambda_i^{1/3} \cdot e^{\frac{2\pi i}{3}}, \lambda_i^{1/3} \cdot e^{\frac{4\pi i}{3}}\}$. This is an exact relation for any N and follows from the relation between the resolvents (here the matrices A_i are of *finite size* and *fixed i.e.* no averaging)

$$G_{\mathcal{B}_3}(w) = \frac{1}{3N} \text{tr} \frac{1}{w - \mathcal{B}_3}, \quad G_{A_1A_2A_3}(z) = \frac{1}{N} \text{tr} \frac{1}{z - A_1A_2A_3}
 \tag{48}$$

namely

$$wG_{\mathcal{B}_3}(w) = zG_{A_1A_2A_3}(w^3 \equiv z).
 \tag{49}$$

This is due to the cyclic structure of the block matrix (47). Obviously, only multiplicities of the cubic powers of \mathcal{B}_3 contribute to the trace.

The relation between the eigenvalues now follows from the location of the *finite* number of poles of both functions.

We can thus safely calculate the eigenvalue density for the block matrix \mathcal{B}_3 using diagrammatic methods and then extract the density for the product through

$$\rho_{A_1A_2\dots A_M}(z, \bar{z}) = \frac{1}{\pi} \partial_{\bar{z}} G_{A_1A_2\dots A_M} = \frac{1}{M} \frac{w\bar{w}}{z\bar{z}} \rho_{\mathcal{B}_M}(w, \bar{w}),
 \tag{50}$$

where $M = 3$ and $w^M = z$ and $\rho_{\mathcal{B}_M}(w, \bar{w}) = \frac{1}{\pi} \partial_{\bar{w}} G_{\mathcal{B}_M}(w, \bar{w})$.

To extract only the moments involving powers of the triples $A_1A_2A_3$, we construct an auxiliary $6N$ by $6N$ Green’s function, triplicating the $A_1A_2A_3$

products by rewriting them as cyclic block matrices:

$$\mathcal{G}(w) = \left\langle \left[\begin{pmatrix} \mathbf{w} & -\mathbf{1} & 0 & 0 & 0 & 0 \\ 0 & \mathbf{w} & -\mathbf{1} & 0 & 0 & 0 \\ -\mathbf{1} & 0 & \mathbf{w} & 0 & 0 & 0 \\ 0 & 0 & 0 & \bar{\mathbf{w}} & 0 & -\mathbf{1} \\ 0 & 0 & 0 & -\mathbf{1} & \bar{\mathbf{w}} & 0 \\ 0 & 0 & 0 & 0 & -\mathbf{1} & \bar{\mathbf{w}} \end{pmatrix} - \sqrt{\frac{\tau}{3}} \begin{pmatrix} 0 & X_1 & 0 & 0 & 0 & 0 \\ 0 & 0 & X_2 & 0 & 0 & 0 \\ X_3 & 0 & 0 & 0 & 0 & 0 \\ 0 & 0 & 0 & 0 & 0 & X_3^\dagger \\ 0 & 0 & 0 & X_1^\dagger & 0 & 0 \\ 0 & 0 & 0 & 0 & X_2^\dagger & 0 \end{pmatrix} \right]_{6N \times 6N}^{-1} \right\rangle, \quad (51)$$

where we separated the “deterministic” part from the “random one”. Introducing now the block-trace operation tr_{B_6} , we obtain a 6 by 6 auxiliary Green’s function $g(w) = \text{tr}_{B_6} \mathcal{G}(w)$. In such a way we again managed to *linearize* the problem, at the cost of increasing the size of the matrices.

The generalization for arbitrary M is now straightforward. For

$$Y_M = \left(1 + \sqrt{\frac{\tau}{M}} X_1 \right) \left(1 + \sqrt{\frac{\tau}{M}} X_2 \right) \dots \left(1 + \sqrt{\frac{\tau}{M}} X_M \right) \quad (52)$$

we define an auxiliary $2MN$ by $2MN$ Green’s function of the form

$$\mathcal{G}(w) = \left\langle \left(\begin{pmatrix} \mathbf{w} & -\sqrt{\frac{\tau}{M}} \mathcal{X} \\ -\sqrt{\frac{\tau}{M}} \mathcal{X}^\dagger & \mathbf{w}^\dagger \end{pmatrix} \right)^{-1} \right\rangle. \quad (53)$$

The structure of the blocks in this matrix originates from complex replication method introduced in the previous chapter. Each of the blocks is then farther linearized using the cyclic properties of the matrices, *i.e.* blocks read

$$\mathbf{w} = \begin{pmatrix} \mathbf{w} & -\mathbf{1} & 0 & \dots & 0 \\ 0 & \mathbf{w} & -\mathbf{1} & \dots & 0 \\ \dots & \dots & \dots & \dots & \dots \\ 0 & 0 & \dots & \mathbf{w} & -\mathbf{1} \\ -\mathbf{1} & 0 & \dots & 0 & \mathbf{w} \end{pmatrix}_{MN \times MN} \quad (54)$$

and

$$\mathcal{X} = \begin{pmatrix} 0 & X_1 & 0 & \dots & 0 \\ 0 & 0 & X_2 & \dots & 0 \\ \dots & \dots & \dots & \dots & \dots \\ 0 & 0 & \dots & 0 & X_{M-1} \\ X_M & 0 & \dots & 0 & 0 \end{pmatrix}_{MN \times MN} \quad (55)$$

are themselves NM by NM matrices, *i.e.* each of the listed elements in \mathcal{W} and in \mathcal{X} is itself an N by N matrix, either diagonal, denoted by a bold symbol, or a random entry X_i , otherwise an N by N block of zeroes.

We take now a block-trace operation tr_{BM} , where we trace each N by N block of the $2MN$ by $2MN$ matrix $\mathcal{G}(w)$ separately. In such a way, we obtain a $2M$ by $2M$ auxiliary Green’s function

$$\begin{aligned}
 g(w) &\equiv \begin{pmatrix} g_{11} & \cdots & g_{1M} & g_{1\bar{1}} & \cdots & g_{1\bar{M}} \\ \vdots & \ddots & \vdots & \vdots & \ddots & \vdots \\ g_{M1} & \cdots & g_{MM} & g_{M\bar{1}} & \cdots & g_{M\bar{M}} \\ g_{\bar{1}1} & \cdots & g_{\bar{1}M} & g_{\bar{1}\bar{1}} & \cdots & g_{\bar{1}\bar{M}} \\ \vdots & \ddots & \vdots & \vdots & \ddots & \vdots \\ g_{\bar{M}1} & \cdots & g_{\bar{M}M} & g_{\bar{M}\bar{1}} & \cdots & g_{\bar{M}\bar{M}} \end{pmatrix}_{2M \times 2M} \\
 &= \frac{1}{N} \text{Tr}_{BM} \mathcal{G}(w). \tag{56}
 \end{aligned}$$

As before we define a $2M$ by $2M$ matrix of self-energies $\tilde{\Sigma}_{ij}$

$$g(w) = \left[\begin{pmatrix} \mathcal{W} & 0 \\ 0 & \mathcal{W}^\dagger \end{pmatrix} - \tilde{\Sigma} \right]^{-1}, \tag{57}$$

where \mathcal{W} is a result of block-tracing \mathcal{W} . We can now diagrammatically analyze the content of the matrix $\tilde{\Sigma}$. As previously, only “double line” propagators $\langle X_i X_i^\dagger \rangle_{X_i}$ for $i = 1, \dots, M$ are different from zero. Therefore, from all of the $4M^2$ elements of the matrix $\tilde{\Sigma}$ only $2M$ are different from zero. Due to the symmetries we get

$$\begin{aligned}
 \Sigma_{1\bar{1}} &= \dots = \Sigma_{M\bar{M}} = \alpha g_{\bar{1}1} = \alpha g_{\bar{M}M} \equiv \alpha g, \\
 \Sigma_{\bar{1}1} &= \dots = \Sigma_{\bar{M}M} = \alpha g_{1\bar{1}} = \alpha g_{1\bar{M}} \equiv \alpha \tilde{g}, \tag{58}
 \end{aligned}$$

where the factor $\alpha = \tau/M$ comes from the propagator in the corresponding set of Schwinger–Dyson equations as in the previous chapter.

Inserting now the matrix $\tilde{\Sigma}$ with entries (58) we arrive at a $2M$ by $2M$ matrix equation for the elements of the Green’s function. First, we solve it for g and \tilde{g} . Second, using the solutions, we calculate g_{11} . Third, using (50) we get an explicit equation for the spectral density

$$\rho(x, y) = \frac{1}{\pi} \frac{1}{M} \frac{w\bar{w}}{z\bar{z}} \partial_{\bar{w}} g_{11}(w, \bar{w}), \tag{59}$$

where $z = x + iy$. For arbitrary M , the algebra is rather involved. Luckily, both the block and the cyclic structure of the main entries \mathcal{W} and $\tilde{\Sigma}$ make

taking an inverse of the $2M$ by $2M$ matrix possible. The inverse of a cyclic matrix is a cyclic matrix, and its explicit form can be obtained from the solution of an associated recurrence relation, *e.g.* using the transfer matrix techniques.

We skip here the intermediate calculations, referring to the original paper [44]. We present here the final solution of the shape of the curve bordering the complex eigenvalues as a function of the evolution time τ . Explicit solution for the boundary is surprisingly simple and reads

$$\frac{\tau}{2} \left(\frac{r^2 - 1}{\ln r} \right) = r^2 + 1 - 2r \cos \phi, \tag{60}$$

where we used polar decomposition $z = r \exp i\phi$. We would like to stress, that in the limit of infinitely many products (*i.e.* $M \rightarrow \infty$) the shape of the boundary acquired a new symmetry — (60) is invariant under inversion operation $r \rightarrow 1/r$. This symmetry is responsible for the appearance of a structural change of the spectrum — provided τ is sufficiently large, *two* boundaries, related by inversion in the radial variable, appear. We describe this structural change of the complex spectrum as a “topological phase transition”. The spectral density as a function of t could be easily inferred from the formulae in [44].

As a confirmation of our analytical predictions, we performed some numerical simulations. Figure 4 shows the evolution of the boundary for several sample evolution times $\tau = 0.5, 1, 1.5, 2, 3, 4, 5, 6, 8, 12$. To present the whole set of the boundaries on the same figure, each boundary is rescaled by a corresponding factor $\exp(-\tau/2)$. We would like to note here that the effect of rescaling is equivalent to the non-rescaled process with drift $\mu = 1$. One can see how the original ellipse-like shape (innermost figure) evolves through a twisted-like shape to the set of double-ring structures. The inner ring, always containing the origin, is so small on the scale of the Fig. 4 that it is not visible. At $\tau = 4$, corresponding to the curve with an inner loop, we observe a topological phase transition. The support of the spectrum is no longer simply connected, for $\tau \geq 4$ it is annulus-like, *i.e.* eigenvalues are expelled from the central region. For even larger times, the outside rim of the annulus approaches the circle, and the inner one shrinks to the point $z = 0$ in the $\tau = \infty$ limit. Indeed for large τ the radius of the inner ring behaves like

$$r(\tau) \sim e^{-\frac{\tau}{2}}. \tag{61}$$

The outer boundary then forms approximately a circle with the radius $e^{\tau/2}$. To visualize the repulsion of the eigenvalues from the region around $z = 0$ we performed higher statistics simulations for $\tau = 4$, corresponding to Fig. 5. Note that the eigenvalue distributions are quite high for small z and the size

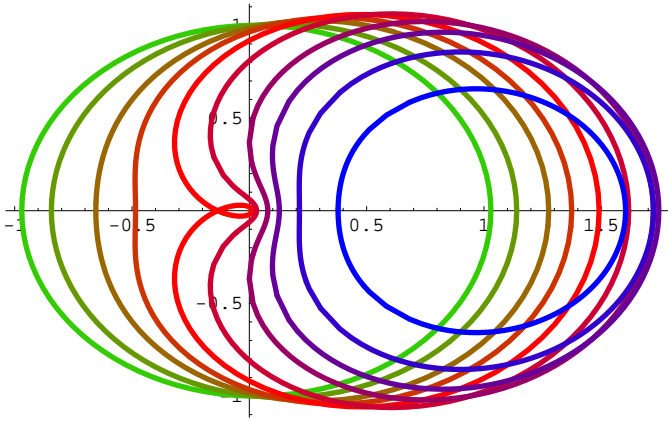


Fig. 4. Evolution of the rescaled (see text) contour of non-holomorphic domain in the eigenvalue spectrum of the Ginibre–Girko multiplicative diffusion as a function of several times τ .

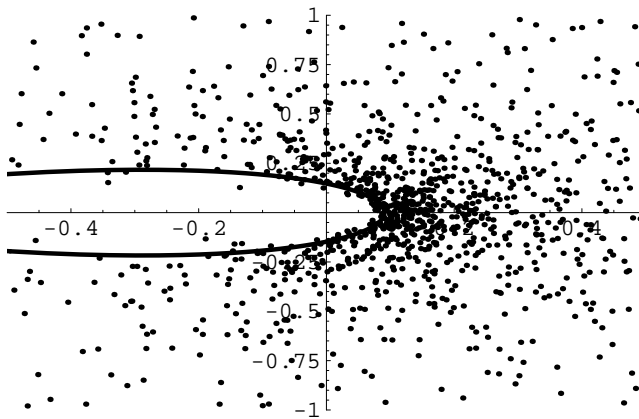


Fig. 5. Comparison of the analytical contour for the eigenvalue spectrum of Ginibre–Girko multiplicative diffusion at evolution time $\tau = 4$, versus the high-statistics numerical simulation of the spectrum.

of the inner ring is indeed very small. Therefore it is quite difficult to observe numerically the exact exclusion of eigenvalues from the marked region.

Figure 6 shows the comparison of numerically generated eigenvalues versus the analytical prediction of the shape of the support of eigenvalues of the “evolution operator”. Again, the same rescaling by $\exp(-\tau/2)$ was applied.

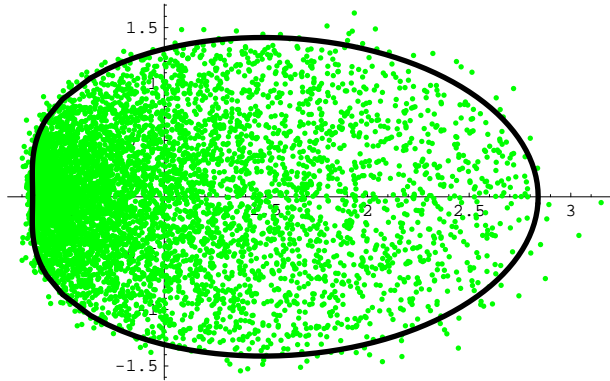


Fig. 6. Comparison of the analytical contour for the eigenvalue spectrum of Ginibre–Girko multiplicative diffusion at evolution time $\tau = 1.$, versus the numerical simulation of the spectrum. The generated ensemble consisted of 60 matrices, each for $N = M = 100$. Note that the vertical axis is located at $x = 1$ and not at $x = 0$. The origin lies outside the figure.

5. Conclusions

We have introduced a natural generalization of the concept of geometric random walk (‘geometric diffusion’) in the space of large, non-commuting matrices. Using diagrammatic methods combined with ‘complex replication’ and ‘cyclization’ tricks, we obtained an explicit solution for the evolution of the spectral domain in the case of Ginibre–Girko type of diffusion.

We observed, that the spectrum develops a surprising feature, namely a region *without* eigenvalues appears within the spectrum after a finite nonzero evolution time has elapsed, thus changing its topological properties. We can thus describe this behavior as a topological phase transition. This points at the appearance of a particular *repulsion* mechanism for sufficiently large evolution times, which, under the unfolding procedure, will turn out most probably to be of a novel *universal* class.

One of the motivations for this work was to propose a general formalism, which can provide a straightforward method of analyzing spectral properties of multivariate diffusion-like processes, with the idea that our method could be used in different branches of theoretical physics and interdisciplinary applications. The particular diffusion process discussed here could be generalized for other cases of matrix-valued random processes [44, 45].

Last but not least, the presented formalism can be viewed as a starting point for establishing a direct link [45] to the diffusion processes based on Free Random Variables techniques [40, 41, 46], allowing for several new surprising analogies between the classical and non-commutative probability calculi.

This work was partially supported by the Polish State Committee for Scientific Research (KBN) grants 2P03B 09622 (2002-2004), 2P03B08225 (2003-2006) and the EU network HPRN CT 1999-00161. The authors would like to thank Angelo Vulpiani for interesting discussions. We are also very grateful to Roland Speicher and Piotr Śniady for valuable remarks in relation to Free Random Variable calculus.

REFERENCES

- [1] see *e.g.* M.L. Mehta, *Random Matrices*, Academic Press, New York, 1991; C.E. Porter, *Statistical Theories of Spectra: Fluctuations*, Academic Press, New York, 1969.
- [2] N. Dupuis, G. Montambaux, *Phys. Rev.* **B43**, 14390 (1991).
- [3] T. Guhr, A. Mueller-Groeling, H.A. Weidenmueller, *Phys. Rep.* **299**, 189 (1998) and references therein.
- [4] F. Haake *et al.*, *Z. Phys.* **B88**, 359 (1992); N. Lehmann, D. Saher, V.V. Sokolov, H.-J. Sommers, *Nucl. Phys.* **A582**, 223 (1995).
- [5] J.J.M. Verbaarschot, I. Zahed, *Phys. Rev. Lett.* **70**, 3852 (1993).
- [6] R. Dijkgraaf, C. Vafa, [hep-th/0208048](https://arxiv.org/abs/hep-th/0208048).
- [7] J. Ambjørn, J. Jurkiewicz, Yu.M. Makeenko, *Phys. Lett.* **B251**, 517 (1990).
- [8] J. Ambjørn, L. Chekhov, C.F. Kristjansen, Yu. Makeenko, *Nucl. Phys.* **B404**, 127 (1993).
- [9] see P. Di Francesco, P. Ginsparg, J. Zinn-Justin, *Phys. Rept.* **254**, 1 (1995), and references therein.
- [10] M.S. Santhanam, P.K. Patra, *Phys. Rev.* **E64**, 016102 (2001).
- [11] A.M. Sengupta, P.P. Mitra, *Phys. Rev.* **E60**, 3389 (1999).
- [12] H. Caswell, *Matrix Population Models*, Sinauer Ass. Inc, Sunderland, MA 2001.
- [13] R. Mantegna, H. Stanley, *An Introduction in Econophysics*, Cambridge University Press, 2000.
- [14] J.P. Bouchaud, M. Potters, *Theory of Financial Risks*, Cambridge University Press, 2001.
- [15] Z. Burda, J. Jurkiewicz, M.A. Nowak, *Acta Phys. Pol. B* **34**, 87 (2003).
- [16] A. Crisanti, G. Paladin, A. Vulpiani, *Products of Random Matrices in Statistical Physics*, Springer Verlag, Berlin 1993.
- [17] C.W.J. Beenakker, in: *Transport Phenomena in Mesoscopic Systems*, Springer Series in Solid State Sciences, Vol. 109, ed. by H. Fukuyama and T. Ando, (Springer, Berlin 1992).
- [18] X.R. Wang, *J. Phys.* **A29**, 3053 (1996).
- [19] F.K. Diakonov, D. Pingel, P. Schmelcher, *Phys. Rev.* **E62**, 4413 (2000).
- [20] M.J. de Oliveira, A. Petri, *Phys. Rev.* **E53**, 2960 (1996).
- [21] D. Gross, A. Matytsin, *Nucl. Phys.* **B437**, 541 (1995).

- [22] L.D. Paniak, *Nucl. Phys.* **B553**, 583 (1999).
- [23] D. Tse, O. Zeitouni, *IEEE Trans. Inform. Theory* **46**, 172 (2000).
- [24] M.F. Barnsley, in *The Science of Fractal Images*, ed. by H.O. Peitgen and D. Saupe, Springer Verlag, Berlin 1988.
- [25] A.D. Jackson, B. Lautrup, P. Johansen, M. Nielsen, *Phys. Rev.* **E66**, 066124 (2002).
- [26] I.E. Telatar, *Eur. Trans. Telecommun.* **10**, 585 (1999).
- [27] R.R. Müller, *IEEE Trans. Inform. Theory* **48**, 2495 (2002).
- [28] H.M. Taylor, S. Karlin, *An Introduction to Stochastic Modeling*, Academic Press, NY 1998, 3rd edition.
- [29] E. Brézin, A. Zee, *Phys. Rev.* **E49**, 2588 (1994); E. Brézin, A. Zee, *Nucl. Phys.* **B453**, 531 (1995).
- [30] G. 't Hooft, *Nucl. Phys.* **B75**, 464 (1974).
- [31] R.A. Janik, M.A. Nowak, G. Papp, J. Wambach, I. Zahed, *Phys. Rev.* **E55**, 4100 (1997); R.A. Janik, M.A. Nowak, G. Papp, I. Zahed, *Nucl. Phys.* **B501**, 603 (1997). A different, but equivalent approach was also developed by [32].
- [32] J. Feinberg, A. Zee, *Nucl. Phys.* **B501**, 643 (1997); J. Feinberg, A. Zee, *Nucl. Phys.* **B504**, 579 (1997); J.T. Chalker, Z. Jane Wang, *Phys. Rev. Lett.* **79**, 1797 (1997); Y.V. Fyodorov, H.-J. Sommers, unpublished.
- [33] E. Wigner, *Can. Math. Congr. Proc.* University of Toronto Press, p.174 and other papers reprinted in C.E. Porter *Statistical Theories of Spectra: Fluctuations*, Academic Press, New York 1965.
- [34] J. Ginibre, *J. Math. Phys.* **6**, 440 (1965).
- [35] V.L. Girko, *Spectral Theory of Random Matrices* (in Russian), Nauka, Moscow (1988) and references therein.
- [36] L.G. Brown, *Geometric Methods in Operator Algebras*, Longman Sci. Tech., Harlow 1986, p. 1.
- [37] U. Haagerup, F. Larsen, *J. Funct. Anal.* **176(2)**, 331 (2000).
- [38] P. Śniady, *J. Funct. Anal.* **193(2)**, 291 (2002).
- [39] Y.V. Fyodorov, H.-J. Sommers, *J. Math. Phys.* **38**, 1918 (1997); Y.V. Fyodorov, B.A. Khoruzhenko, H.-J. Sommers, *Phys. Lett.* **A226**, 46 (1997); H.-J. Sommers, A. Crisanti, H. Sompolinsky, Y. Stein, *Phys. Rev. Lett.* **60**, 1895 (1988).
- [40] D. Voiculescu, *Invent. Math.* **104**, 201 (1991); D.V. Voiculescu, K.J. Dykema, A. Nica, *Free Random Variables*, Am. Math. Soc., Providence, RI, 1992.
- [41] R. Speicher, *Math. Ann.* **298**, 611 (1994).
- [42] R.A. Janik, W. Noerenberg, M.A. Nowak, G. Papp, I. Zahed, *Phys. Rev.* **E60**, 2699 (1999).
- [43] E. Gudowska-Nowak, G. Papp, J. Brickmann, *Chem. Phys.* **232**, 247 (1998).
- [44] E. Gudowska-Nowak, R.A. Janik, J. Jurkiewicz, M.A. Nowak, math-ph/0304032, *Nucl. Phys.* **B** (in press).
- [45] in preparation.
- [46] Ph. Biane, R. Speicher, *Ann. Inst. Henri Poincaré — PR* **37 (5)**, 581 (2001).